JACC: BASIC TO TRANSLATIONAL SCIENCE VOL. 9, NO. 6, 2024

ORIGINAL RESEARCH - PRECLINICAL

Fibroblast-Specific Depletion of Human Antigen R Alleviates Myocardial Fibrosis Induced by Cardiac Stress

Mallikarjun Patil, PhD,[a,*] Sarojini Singh, PhD,[a,*] Praveen Kumar Dubey, PhD,[a] Sultan Tousif, PhD,[b] Prachi Umbarkar, PhD,[b] Qinkun Zhang, MD,[b] Hind Lal, PhD,[b] Mary Kathryn Sewell-Loftin, PhD,[a] Channakeshava Sokke Umeshappa, PhD,[c] Yohannes T. Ghebre, PhD,[d] Steven Pogwizd, MD,[e] Jianyi Zhang, MD, PhD,[a] Prasanna Krishnamurthy, PhD[a]

VISUAL ABSTRACT

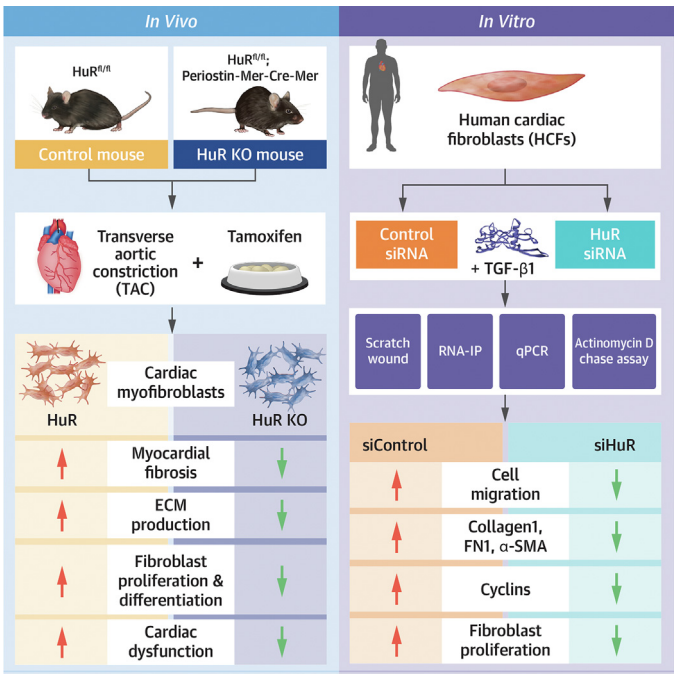

Patil M, et al. J Am Coll Cardiol Basic Trans Science. 2024;9(6):754–770.

HIGHLIGHTS

- **HuR, an RNA-binding protein, plays a critical role in organ fibrosis across various pathologies.**
- **A novel conditional tamoxifen-inducible HuR knockout mouse enabled the deletion of HuR from activated fibroblasts after cardiac injury.**
- **Myofibroblast-specific deletion of HuR significantly limited cardiac fibrosis and preserved cardiac function in pressure overload injury.**
- **HuR promotes myofibroblast proliferation by regulating the messenger RNA expression and stability of cyclins D1 and A2, and deletion of HuR reduced the proliferation of activated fibroblasts.**

From the [a]Department of Biomedical Engineering, Heersink School of Medicine and School of Engineering, University of Alabama at Birmingham, Birmingham, Alabama, USA; [b]Division of Cardiovascular Disease, Heersink School of Medicine, University of Alabama at Birmingham, Birmingham, Alabama, USA; [c]Department of Microbiology and Immunology, Dalhousie University, Halifax, Nova Scotia, Canada; [d]Department of Radiation Oncology, the University of Texas Health Science Center at San Antonio, San Antonio, Texas, USA; and the [e]Comprehensive Cardiovascular Center, Department of Medicine, University of Alabama at Birmingham, Birmingham, Alabama, USA. *Drs Patil and Singh contributed equally to this work and are joint first authors.
The authors attest they are in compliance with human studies committees and animal welfare regulations of the authors' institutions and Food and Drug Administration guidelines, including patient consent where appropriate. For more information, visit the Author Center.

Manuscript received December 22, 2023; revised manuscript received March 4, 2024, accepted March 5, 2024.

ISSN 2452-302X https://doi.org/10.1016/j.jacbts.2024.03.004

SUMMARY

Cardiac fibrosis can be mitigated by limiting fibroblast-to-myofibroblast differentiation and proliferation. Human antigen R (HuR) modulates messenger RNA stability and expression of multiple genes. However, the direct role of cardiac myofibroblast HuR is unknown. Myofibroblast-specific deletion of HuR limited cardiac fibrosis and preserved cardiac functions in pressure overload injury. Knockdown of HuR in transforming growth factor-β1-treated cardiac fibroblasts suppressed myofibroblast differentiation and proliferation. HuR deletion abrogated the expression and messenger RNA stability of cyclins D1 and A2, suggesting a potential mechanism by which HuR promotes myofibroblast proliferation. Overall, these data suggest that inhibition of HuR could be a potential therapeutic approach to limit cardiac fibrosis. (J Am Coll Cardiol Basic Trans Science 2024;9:754–770)

ABBREVIATIONS AND ACRONYMS

α-SMA = α-smooth muscle actin

3′-UTR = 3′-untranslated region

ARE = adenylate-uridylate–rich elements

BrdU = 5-bromo-2′-deoxyuridine

CCNB1 = cyclin B1

CCND1 = cyclin D1

CCNE1 = cyclin E1

CCNA2 = cyclin A2

CT = control

Elavl1 = ELAV (Embryonic Lethal, Abnormal Vision, Drosophila)-Like 1

HCF = human cardiac fibroblast

HuR = human antigen R

IgG = immunoglobulin G

IL = interleukin

KO = knockout

LV = left ventricular

mRNA = messenger RNA

qRT-PCR = quantitative reverse transcription polymerase chain reaction

PBS = phosphate-buffered saline

PDGFR = platelet-derived growth factor receptor

RBP = RNA-binding protein

siHuR = human antigen R small interfering RNA

TAC = transverse aortic constriction

TGF = transforming growth factor

Cardiac fibrosis is a hallmark of heart failure, characterized by the activation and expansion of resident fibroblasts and excessive accumulation of extracellular matrix components.[1,2] Uncontrolled fibrosis leads to scarring and stiffness of the heart, accompanied by compromised systolic and diastolic function. Cardiac fibroblasts primarily drive fibrosis by differentiating into myofibroblasts, inducing extracellular matrix production.[2,3] The fibroblast-to-myofibroblast conversion is a dynamic process, tightly regulated at both the transcription and translation level during the fibrotic response.[4] RNA-binding proteins (RBPs) regulate hundreds of genes and are continuously gaining attention in the pathogenesis of fibrosis, including cardiac fibrosis.[4-6] Fibroblasts, the second major cell type in the heart, are required to maintain heart architecture, functions, and overall cardiac homeostasis. Fibroblasts differentiate into myofibroblasts in response to various cardiac stressors, initiating a fibrotic response. Despite substantial knowledge of fibrosis-inflicted cardiac remodeling and dysfunction, effective antifibrotic therapies and interventions to halt or reverse fibrosis progression are limited.[7] It is therefore necessary to explore and develop effective antifibrotic strategies.

Human antigen R (HuR) (*Elavl1*) is a ubiquitously expressed RBP that binds to adenylate-uridylate-rich elements (ARE) in the 3′-untranslated region (3′-UTR) of targeted messenger RNAs (mRNAs), regulating their stability and translation.[8-11] HuR has been identified as a regulator of organ fibrosis, such as liver,[12] renal,[13] and lung[14] fibrosis. Literature has highlighted the potential involvement of HuR in myocardial remodeling.[15-17] Our laboratory has shown that macrophage-associated HuR promotes fibroblast-to-myofibroblast differentiation and cardiac fibrosis in diabetic hearts through exosomes.[18] Furthermore, inhibition of HuR attenuates cardiac inflammation and remodeling in myocardial infarction[17] and cardiac pressure overload[15] mouse models. Green et al[19] recently showed that HuR is directly involved in the transforming growthfactor(TGF)-β1-mediated activation of cardiac myofibroblast by posttranscriptional modulation of WISP-1, an extracellular matrix-associated signaling protein, endorsing the role of HuR in myofibroblast function. In concordance with this study, we also found that HuR augmented fibroblast-to-myofibroblast differentiation in vitro. These studies indicate that HuR could be a potential therapeutic target to curtail detrimental fibrotic outcomes in cardiac injuries.

Developments in the generation of fibroblast-specific Tcf21^{MCM} and Postn^{MCM} mouse models have enabled the effective manipulation of target genes in tissue-resident fibroblasts and myofibroblasts, respectively.[20-25] In the current study, we generated a tamoxifen-inducible periostin-Cre-driven myofibroblast-specific HuR knockout mouse to delete HuR from activated fibroblasts. As shown in the Postn^{MCM} model, periostin-Cre is activated in fibroblasts only after stress; this model therefore closely mimics the clinical scenario in which patients present following the onset of disease. We observed that myofibroblast-specific HuR deletion protected against fibrotic remodeling and cardiac dysfunction in a transverse aortic constriction (TAC) model. Moreover, 5-bromo-2′-deoxyuridine (BrdU) incorporation studies revealed a reduction in myofibroblast population in HuR knockout (KO) mice subjected to

JACC: BASIC TO TRANSLATIONAL SCIENCE VOL. 9, NO. 6, 2024
JUNE 2024:754–770

pressure overload compared with control (CT) mice. Further investigation revealed that HuR modulated the expression and mRNA stability of cyclins in TGF-β1-treated human cardiac fibroblasts (HCFs), potentially affecting myofibroblast proliferation. In summary, the RBP HuR significantly influences the ability of cardiac fibroblasts to promote myocardial fibrosis. Therefore, targeting HuR in activated fibroblasts represents a promising therapeutic approach to restrict myocardial fibrosis.

METHODS

MICE. Mouse colonies were maintained under a standard vivarium condition with a 12-hour light/12-hour dark cycle and provided with food and water ad libitum. To generate myofibroblast-specific HuR knockout mice, we crossed $HuR^{fl/fl}$ (B6.129-$Elavl1^{tm1Thla}$/J, stock no. 021431; The Jackson Laboratory) mice[26] with Periostin-Mer-Cre-Mer (B6.129S-$Postn^{tm2.1(cre/Esr1*)Jmol}$/J, stock no. 029645; The Jackson Laboratory) mice.[24] The resulting $HuR^{fl/fl/Cre+/-}$/tamoxifen mice were used as myofibroblast-specific HuR KO mice; their littermates, $HuR^{fl/fl/Cre-/-}$/tamoxifen mice, were designated as CT mice. The mice were born healthy and were fertile.

All animal procedures were approved by the Institutional Animal Care and Use Committee of the University of Alabama at Birmingham.

TAC SURGERY. TAC was performed as described previously.[27] Briefly, 12-week-old mice were fed a tamoxifen diet (catalog no. TD.130860; Envigo) 2 weeks before TAC surgery and were maintained on a tamoxifen diet for 8 more weeks. The mice were returned to a regular diet of chow for 36 hours before TAC surgery to avoid increased mortality. For TAC, mice were anesthetized with ketamine (50 mg/kg, intraperitoneally) and xylazine (2.5 mg/kg, intraperitoneally). Anesthetized mice were intubated and ventilated through a volume-cycled rodent ventilator on supplemental oxygen at a rate of 1 L/min with a respiratory rate of 140 breaths/min. Aortic constriction was achieved by tying down the aorta using a 7-0 nylon suture ligature against a 27-gauge needle. The needle was then promptly removed to yield a constriction of approximately 0.4 mm in diameter. The animals were monitored until complete recovery. A sham operation was similarly conducted without suture ligation. After surgery, the mice were provided a postoperative gel diet for 24 hours and then fed a tamoxifen diet until the end of the study.

TWO-DIMENSIONAL ECHOCARDIOGRAPHY. Mice were anesthetized with a mixture of 1.5% isoflurane and oxygen (1 L/min), and transthoracic two-dimensional echocardiography was performed by using Vevo 2100 (VisualSonics) as described previously.[28] Left ventricular (LV) internal dimensions (LV internal diameter end-systole and end-diastole), ejection fraction, fractional shortening, and other echocardiographic parameters were recorded at baseline and 8 weeks after TAC.

HISTOLOGIC ANALYSIS. At endpoint, animals were sacrificed, and the heart was removed immediately. Heart tissues were fixed in 10% neutral-buffered formalin, embedded in paraffin, and heart sections of 5 μm thickness were prepared. Hematoxylin and eosin (catalog no. H-3502; Vector Laboratories) and Masson trichrome (catalog no. HT15; Sigma-Aldrich) staining was performed on the heart sections as per the manufacturers' instructions. The images of the LV region were captured under a Nikon Eclipse E200 microscope with NIS-Elements software version 4.60 (Nikon Instruments). A minimum of 150 to 250 cardiomyocytes from each mouse per group was traced for the measurement of cardiomyocyte cross-sectional area. For fibrosis measurement, 6 to 8 images of the LV region of the Masson trichrome–stained sections were captured. The quantification of LV fibrosis and cross-sectional area of cardiomyocytes was determined by using ImageJ software (National Institutes of Health) from captured images.

RNA EXTRACTION AND REAL-TIME QUANTITATIVE POLYMERASE CHAIN REACTION ANALYSIS. Total RNA was extracted by using an RNA extraction kit (RNeasy Mini Kit, catalog no. 74104; Qiagen) according to the manufacturer's instructions. The RNA was reverse transcribed to complementary DNA using the RevertAid First Strand cDNA Synthesis Kit (catalog no. K1622; Thermo Fisher Scientific). Real-time quantitative polymerase chain reaction (qPCR) was performed in a QuantStudio 3 system (Applied Biosystems) using PowerUp SYBR Green Master Mix (catalog no. A25778; Thermo Fisher Scientific) according to the manufacturer's instructions. Relative mRNA expression was normalized to the housekeeping genes (GAPDH or 18S rRNA). Gene expression was determined by the comparative CT method (ie, $2^{-\Delta\Delta CT}$) and is represented as fold change. The primer sequences of the genes are given in Supplemental Table 1.

IN VIVO BrdU LABELING. For in vivo cardiac fibroblast proliferation assay, mice were intraperitoneally administered BrdU (10 mg/kg body weight in sterile phosphate-buffered saline [PBS]; catalog no. B5002; Sigma-Aldrich) for 3 consecutive days after 1 week of TAC surgery. The hearts were harvested and processed for flow cytometry by using a BrdU labeling

and detection kit (catalog no. 11296736001; Roche) according to the manufacturer's instructions.[27]

FLOW CYTOMETRY. The mice hearts were perfused with ice-cold PBS, harvested, and collected in PBS on ice. The hearts were cut into small pieces and digested in RPMI 1640 containing collagenase type I (1 mg/mL, catalog no. C0130; Sigma-Aldrich), collagenase type XI (0.1 mg/mL, catalog no. C7657; Sigma-Aldrich), hyaluronidase (0.1 mg/mL, catalog no. H3506; Sigma-Aldrich), and DNase I (1 μL/mL, catalog no. D4527; Sigma-Aldrich) at 37°C for 1 hour with gentle shaking. The digestion was stopped using RPMI 1640 with 5% fetal bovine serum and filtered through 70 μm cell strainers. The suspension was centrifuged at 450*g* for 5 minutes and washed with PBS. The pellet was resuspended in fluorescence-activated cell sorting buffer to make a single-cell suspension.

For analysis, cells were blocked with an Fc blocker followed by surface staining (platelet-derived growth factor receptor-α [PDGFR-α], CD45, and CD31) for 30 minutes on ice. After washing with PBS, cells were fixed and permeabilized using the BD Cytofix/Cytoperm kit (BD Biosciences) for 30 minutes at 4°C. The cells were then washed with the BD Perm/Wash kit (BD Biosciences) and stained with intracellular primary antibodies (HuR and α-smooth muscle actin [α-SMA]) followed by fluorescence-tagged secondary antibodies. Dead cells were excluded by using 7-aminoactinomycin D (catalog no. A1310; Thermo Fisher Scientific). Details of antibodies used in this study are provided in Supplemental Table 2. Fluorescence intensity was measured by using BD LSR-II at The University of Alabama at Birmingham Flow Cytometry Core Facility. BD FACSDiva (BD Biosciences) was used for acquiring the cells, and data were analyzed by using FlowJov10.6.1 (TreeStar).[27]

PRIMARY MOUSE CARDIAC FIBROBLASTS ISOLATION. Mouse cardiac fibroblasts were isolated as described previously.[27] Briefly, mice were sacrificed, and the hearts were excised. The hearts were rinsed in cold Krebs-Henseleit buffer (catalog no. K7353; Sigma-Aldrich) supplemented with $CaCl_2$ (2.9 mM, catalog no. C3306; Sigma-Aldrich) and $NaHCO_3$ (24 mM, catalog no. S5761; Sigma-Aldrich). The hearts were minced and serially digested at 37°C in Hanks' balanced salt solution (catalog no. 21-023-CV; Corning) with Liberase TH (0.25 mg/mL, catalog no. 05401151001; Roche), DNase I (20 U/mL, catalog no. D4527; Sigma-Aldrich), and 4-(2-hydroxyethyl)-1-piperazineethanesulfonic acid (10 mmol/L, catalog no. 15630-080; Gibco). After each digestion, suspension was passed through a 40 μm cell strainer and collected in a tube containing Dulbecco's Modified Eagle Medium/Nutrient Mixture F-12 (DMEM/F-12, Thermo Fisher Scientific) with 10% fetal bovine serum. After final digestion, the cell suspension was centrifuged at 1000 rpm for 10 minutes.

Next, the pellet was resuspended in ACK Lysing Buffer (catalog no. A1049201; Gibco) and incubated for 1 minute to lyse red blood cells. The cells were washed with Krebs-Henseleit buffer and centrifuged at 1000 rpm for 10 minutes. The pellet was resuspended in DMEM/F-12 with 10% fetal bovine serum and plated onto culture dishes. After 2 hours, unattached and dead cells were washed with Dulbecco's phosphate-buffered saline, and fresh medium was added to fibroblast culture.

In some experiments, fibroblasts were enriched by using the Magnetic cell isolation and cell separation kit (catalog no. 130-042-301; Miltenyi Biotec) with recommended dilutions of antibodies against CD31 (catalog no. 130-097-418; Miltenyi Biotec) and CD45 (catalog no. 130-052-301; Miltenyi Biotec) as per the manufacturer's instructions.

CELL CULTURE, RNA INTERFERENCE, AND TREATMENTS. Human ventricular cardiac fibroblasts (designated as HCFs; catalog no. CC-2904; Lonza) were cultured in FGM-3 Cardiac Fibroblast Growth Medium-3 BulletKit (catalog no. CC-4526; Lonza) in a humified incubator at 37°C with 5% carbon dioxide.

For RNA interference studies, HCFs were transfected either with HuR small interfering RNA (siHuR; Silencer Select, catalog no. s171151; Thermo Fisher Scientific) or scramble control (siControl; Silencer Select Negative Control#1, catalog no. 4390843; Thermo Fisher Scientific) using Lipofectamine RNAiMAX reagent (catalog no. 13778150; Thermo Fisher Scientific) as per the manufacturer's instructions. HuR knockdown was confirmed by qRT-PCR and Western blot analysis. HCFs were serum-starved (medium containing 0.1% bovine serum albumin) overnight before treatment with TGF-β1 (10 ng/mL, catalog no. 100-21; PeproTech) for the indicated time points.

CELL MIGRATION ASSAY. HCFs were seeded in 6-well culture dishes and transfected with either scrambled small interfering RNA (siControl) or siHuR. The cells were allowed to grow till 90% confluency. The HCF monolayer was then scratched with a 200 μL pipette tip. Cells were treated with TGF-β1 (10 ng/mL, catalog no. 100-21; PeproTech), and images were captured (Olympus CKX53 microscope) at 0, 6, and 12 hours to monitor wound closure. The percentage of wound closure was quantified by using an ImageJ plugin from captured images.[29]

CELL PROLIFERATION ASSAY. HCFs were seeded in 96-well format dishes and transfected with either scrambled small interfering RNA (siControl) or siHuR. After 24 hours, the cells were incubated with TGF-β1–containing medium for an additional 48 hours. After 48 hours, cell proliferation was measured by using the CyQUANT MTT cell proliferation assay kit (catalog no. V13154; Thermo Fisher Scientific) according to the manufacturer's protocol.

mRNA STABILITY ASSAY. mRNA stability of targeted genes was determined by the actinomycin D pulse-chase experiment as described previously.[30] Briefly, HCFs were transfected with either siControl or siHuR and treated with TGF-β1 for 24 hours. The cells were treated with actinomycin D (5 μg/mL, catalog no. A9415; Sigma-Aldrich), and RNA was extracted at 0, 3, and 6 hours after actinomycin D treatment. The expression of genes was examined by qRT-PCR analysis. RNA decay was calculated as the percentage of mRNA remaining over time compared with the amount before the addition of actinomycin D.

RNA IMMUNOPRECIPITATION. HCFs were grown in 150 cm culture dishes up to 80% confluency and washed in RNAse-free PBS. RNA immunoprecipitation was performed[30] by using a RIP-Assay kit (catalog no. RN1001; MBL International) according to the manufacturer's instructions. Briefly, the cells were lysed in cell lysis buffer supplemented with protease and phosphatase inhibitor cocktail, dithiothreitol, and RNaseOUT (Thermo Fisher Scientific) and then centrifuged at 10,000 rpm for 15 minutes at 4°C. The cell extract was transferred into a fresh tube and incubated overnight on a rotator at 4°C with 25 μL of protein A/G magnetic beads (catalog no. 88802; Thermo Fisher Scientific) precoated with either 2 μg of immunoglobulin G (IgG; catalog no. 30000-0-AP; Proteintech) or 2 μg of anti-HuR (catalog no. 11910-1-AP; Proteintech) antibodies. Beads were washed 3 times to remove unbound material. RNA was extracted, reverse-transcribed, and analyzed by qRT-PCR as described earlier.

WESTERN BLOT ANALYSIS. Whole cell protein lysates were prepared in radioimmunoprecipitation assay buffer with a freshly added protease inhibitor cocktail. Protein concentrations were determined by using a protein assay dye (catalog no. 5000006; Bio-Rad) according to the manufacturer's instructions. Equal amounts of proteins were denatured in 4× Laemmli buffer, resolved on denaturing sodium dodecyl sulfate-polyacrylamide gel electrophoresis (4%-20%, Mini-PROTEAN TGX stain-free precast gels; Bio-Rad) and transferred to a polyvinylidene difluoride membrane (Trans-Blot Turbo PVDF transfer system; Bio-Rad). The membranes were blocked with 5% nonfat dry milk (or bovine serum albumin) in tris-buffered saline + Tween 20. The membranes were incubated with primary antibodies followed by horseradish peroxidase–conjugated secondary antibodies and visualized by using an enhanced chemiluminescence (Pierce) detection system. Details of the antibodies used are given in Supplemental Table 2. Images of the blots were acquired by using the ChemiDoc Touch Imaging System (Bio-Rad), and densitometric analyses were performed by using ImageJ software.

COMPUTATIONAL ANALYSIS. Online tools ARED-Plus[31] and AREsite2[32] were used to identify ARE regions in the 3′-UTR of cyclin D1 (CCND1), cyclin A2 (CCNA2), cyclin B1 (CCNB1), and cyclin E1 (CCNE1) mRNA. ViennaRNA Websuite[33] was used to predict HuR-binding sites in 3′-UTR of CCND1 mRNA.

STATISTICAL ANALYSES. Continuous data are presented using the mean ± SEM or median with 25th and 75th percentiles (Q1, Q3) based on data distribution. An unpaired Student's *t*-test, Welch's *t*-test, or two-tailed Mann-Whitney *U* test was performed to determine statistical significance between the 2 groups. Two-way or repeated measures analysis of variance for longitudinal data with a Šidák post hoc test for multiple pairwise comparisons was used for comparisons among multiple groups. A P value <0.05 was considered statistically significant. Statistical analyses were performed by using GraphPad Prism version 10.2.0 (GraphPad Software).

RESULTS

HuR DELETION PREVENTS PHENOTYPIC AND FUNCTIONAL DIFFERENTIATION IN ACTIVATED CARDIAC FIBROBLASTS. TGF-β1 is one of the primary drivers of myofibroblast differentiation and an initiator of fibrosis.[34] Studies have shown that HuR up-regulates TGF-β1 expression by promoting its mRNA stability, and a positive HuR/TGF-β1 feedback loop promotes fibroblast-mediated fibrotic response.[35] To initiate fibroblast activation in vitro, we therefore used exogenous TGF-β1 (10 ng/mL).

Adult mouse cardiac fibroblasts were isolated from C57BL/6 mice and treated with TGF-β1 (10 ng/mL) for 24 hours, which resulted in a significant elevation in HuR expression (**Figure 1A**). Similarly, the transcript level of HuR was also increased in HCFs after TGF-β1 treatment for 24 hours (**Figure 1B**). HCFs were used for further in vitro experiments. Upon activation, fibroblasts acquire hypermigratory and hypercontractile myofibroblast phenotypes; to evaluate the role of HuR in fibroblast-to-myofibroblast differentiation, a

FIGURE 1 Deletion of HuR Prevents Fibroblast-to-Myofibroblast Differentiation in Activated Cardiac Fibroblasts

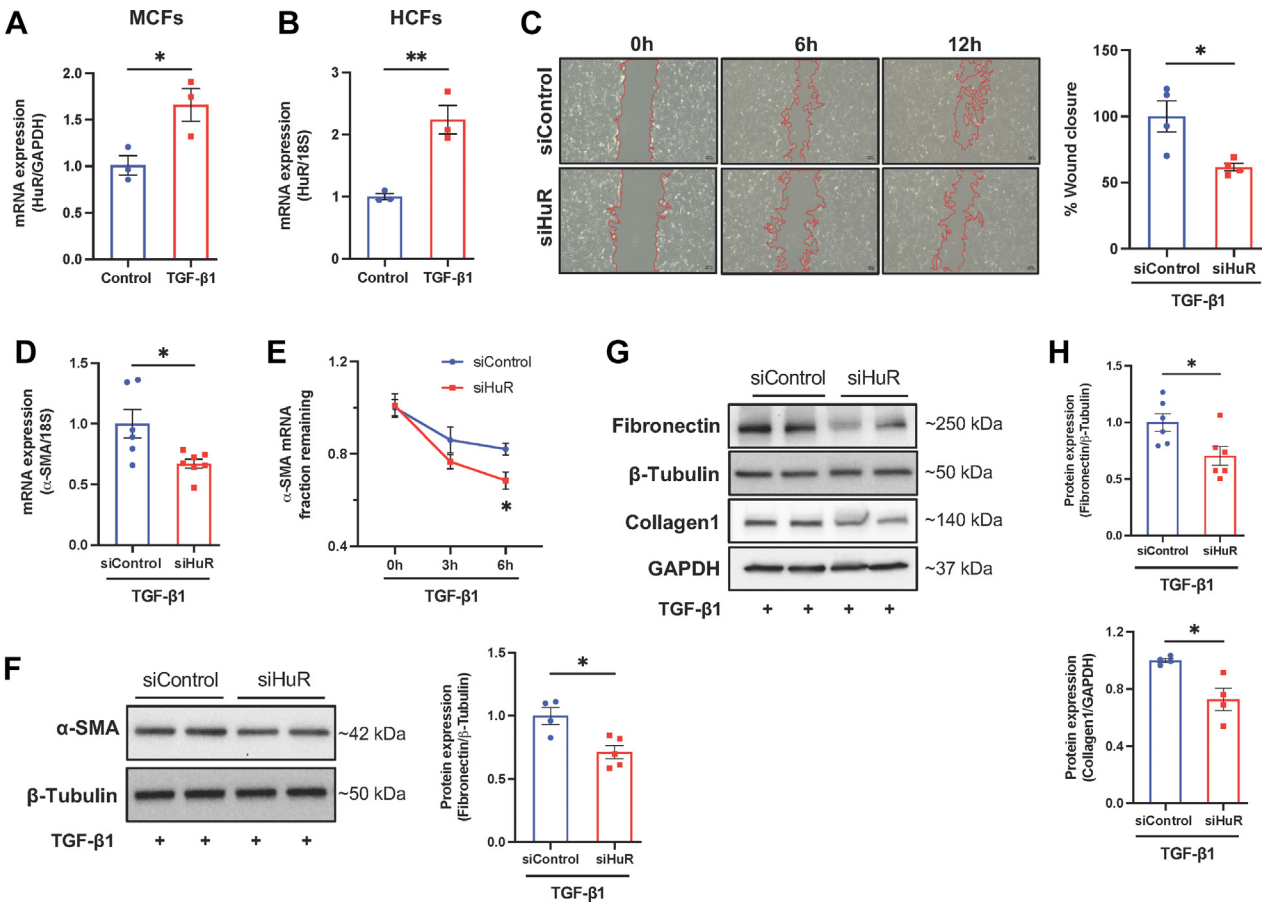

(A) Real-time quantitative polymerase chain reaction analysis of messenger RNA (mRNA) expression of human antigen R (HuR) in primary mouse cardiac fibroblasts (MCFs) stimulated by transforming growth factor(TGF)-β1 (10 ng/mL, 24 hours) normalized to glyceraldehyde 3-phosphate dehydrogenase (GAPDH) (n = 3 per group, *$P < 0.05$ vs control). (B) mRNA expression of HuR in primary human cardiac fibroblasts (HCFs) treated with TGF-β1 (10 ng/mL, 24 hours) normalized to 18S (n = 3 per group, **$P < 0.01$ vs control). (C) Cell migration assay was performed on scramble control (siControl) and HuR knockdown (siHuR) HCFs treated with TGF-β1, and wound closure was monitored. The left panel shows representative images, and the right panel shows quantification of wound closure at 12 hours (n = 4 per group, *$P < 0.05$ vs siControl). (D) mRNA expression of α-smooth muscle actin (SMA) in siControl and siHuR HCFs after TGF-β1 (10 ng/mL, 24 hours) treatment normalized to 18S (siControl, n = 6; siHuR, n = 7; *$P < 0.05$ vs siControl). (E) For mRNA stability of α-SMA, siControl or siHuR HCFs were stimulated with TGF-β1 (10 ng/mL, 24 hours), treated with actinomycin D (5 μg/mL), and RNA decay was analyzed by using real-time quantitative polymerase chain reaction at indicated time points (*$P < 0.05$ vs siControl). (F) Expression of α-SMA in siControl and siHuR HCFs stimulated with TGF-β1 (10 ng/mL, 24 hours). Left panel: representative immunoblots. Right panel: Densitometric analysis of α-SMA normalized to β-tubulin (n = 4-5 per group; *$P < 0.05$ vs siControl). (G) Representative immunoblots for the expression of fibronectin and collagen type I (collagen1) in siControl and siHuR HCFs treated with TGF-β1 (10 ng/mL, 24 hours). β-Tubulin and GAPDH were used as respective loading controls. (H) Densitometric analysis of fibronectin and collagen1 expression (n = 4-6 per group; fibronectin: *$P < 0.05$; collagen1: *$P < 0.05$ vs siControl). Values are mean ± SEM. Data in A, B, F, and H (fibronectin) were analyzed by using an unpaired Student's *t*-test. Data in C, D, and H (collagen1) were compared by using an unpaired Welch's *t*-test. Data in E were analyzed by a two-way repeated measures analysis of variance with a Šidák multiple comparisons test.

cell migration assay was used. For these studies, we silenced HuR in HCFs before stimulation with TGF-β1, and the knockdown efficiency of HuR in HCFs was validated by using real-time qRT-PCR and Western blot analysis (Supplemental Figure 1). For cell migration assay, HuR was knocked down in HCFs, and a scratch wound was created. Control and HuR knockdown HCFs were then treated with 10 ng/mL of TGF-β1 and monitored for wound closure efficiency. As expected, HuR-deficient cardiac fibroblasts

exhibited slower migration than the Control fibroblasts (Figure 1C).

We next examined the expression of α-SMA in siControl and siHuR HCFs after TGF-β1 treatment. The mRNA expression of α-SMA was down-regulated significantly in activated cardiac fibroblasts (Figure 1D). Because HuR enhances the transcription by binding and facilitating the mRNA stability of targeted genes, the mRNA stability of α-SMA was assessed by using an actinomycin D chase assay. After actinomycin D treatment, α-SMA mRNA stability decreased markedly over time in HuR-deficient HCFs (Figure 1E). The protein expression of α-SMA was also down-regulated in the siHuR HCFs compared with the siControl group after TGF-β1 stimulation (Figure 1F). Furthermore, expression of extracellular matrix molecules (fibronectin and collagen type I) was also down-regulated in TGF-β1-treated siHuR HCFs (Figures 1G and 1H) compared with the siControl group. These findings are consistent with a recently published report showing the role of HuR in TGF-β1-induced cardiac fibroblast-to-myofibroblast transformation.[19]

MYOFIBROBLAST-SPECIFIC DELETION OF HuR PRESERVES PRESSURE OVERLOAD–INDUCED LV DYSFUNCTION. Resident cardiac fibroblasts and their transformation into myofibroblasts play a critical role in the resolution of cardiac injury and preservation of heart function. However, sustained activation of myofibroblasts contributes to pathologic fibrosis and the progression of heart failure.[1,2,36] In this study, we investigated the potential of myofibroblast-specific deletion of HuR to limit pathologic cardiac remodeling.

To achieve myofibroblast-specific conditional HuR deletion, we crossed $HuR^{fl/fl}$ mice with Periostin-Mer-Cre-Mer mice, resulting in $HuR^{fl/fl}Postn^{MCM}$ mice (Supplemental Figures 2A and 2B). A tamoxifen diet protocol (described in the Methods section) was used to induce the fibroblast-specific expression of Cre recombinase after TAC injury.[21,27] The pressure gradient across the aortic constriction was measured by using Doppler echocardiography 1 week after surgery to confirm the efficiency of TAC surgery (Supplemental Figure 2C). The resultant myofibroblast-specific HuR knockout mice ($HuR^{fl/fl/Cre+/-}$/tamoxifen) and littermate controls ($HuR^{fl/fl/Cre-/-}$/tamoxifen) were designated as KO and CT mice, respectively (experimental design is shown in Figure 2A). We confirmed the deletion of HuR in $CD45^{-}CD31^{-}PDGFR\text{-}\alpha^{+}$ cardiac fibroblasts of the KO mice through flow cytometry analysis of digested hearts after 8 weeks of TAC (Figure 2B).

Cardiac functions of the CT and KO mice were analyzed by using echocardiography. The baseline cardiac functions were comparable between the 2 groups (Figures 2C and 2D). Importantly, after 8 weeks of TAC, ejection fraction and fractional shortening were preserved in HuR KO mice compared with the CT mice. We also observed a reduction in LV internal dimensions and LV mass in HuR KO mice compared with the CT group (Table 1). These findings suggest that targeting myofibroblast-specific HuR could protect against pressure overload-induced heart failure. Because percent ejection fraction and fractional shortening were comparable between sham groups (Supplemental Figures 2D and 2E), for the rest of the study, we only included experimental analyses for CT and KO mice subjected to TAC surgery. There were no sex-specific cardiac differences between the CT and KO groups (Supplemental Figure 3).

LOSS OF HuR IN MYOFIBROBLASTS RESTRICTS ADVERSE LV FIBROSIS AND REMODELING AFTER CARDIAC STRESS. We next investigated the effect of myofibroblast-specific deletion of HuR on TAC-induced cardiac hypertrophy response. A reduction was observed in the heart weight/tibia length ratio (Figure 3A) and cardiomyocyte cross-sectional area (Figure 3B) in the KO mice compared with the CT mice, although these observations did not reach statistical significance. Interestingly, myofibroblast-specific deletion of HuR significantly reduced the expression of atrial natriuretic peptide and B-type natriuretic peptide (Figures 3C and 3D). These data suggest that deletion of HuR in myofibroblasts may also affect the cardiomyocyte-fibroblast interaction, thereby altering cardiomyocyte biology and function. We next examined the levels of pro-inflammatory cytokines interleukin(IL)-6, IL-1β, and tumor necrosis factor-α in the heart tissues of the CT and KO mice after 8 weeks of TAC surgery. Although the expression of IL-6 and IL-1β was decreased to some extent, no difference was observed in the expression of tumor necrosis factor-α between the CT and HuR KO mice (Supplemental Figure 4).

Masson's trichrome staining was performed to evaluate the extent of cardiac fibrosis. As shown in Figure 4A, cardiac fibrosis was significantly reduced after deletion of HuR. We next examined the population of $PDGFR\text{-}\alpha^{+}\alpha\text{-}SMA^{+}$ fibroblasts in the heart of CT and KO mice by flow cytometry. The reduction in the number of $CD45^{-}CD31^{-}PDGFR\text{-}\alpha^{+}\alpha\text{-}SMA^{+}$ cells in

FIGURE 2 **Myofibroblast-Specific Deletion of HuR Preserves Cardiac Function in Pressure Overload-Induced Cardiac Injury**

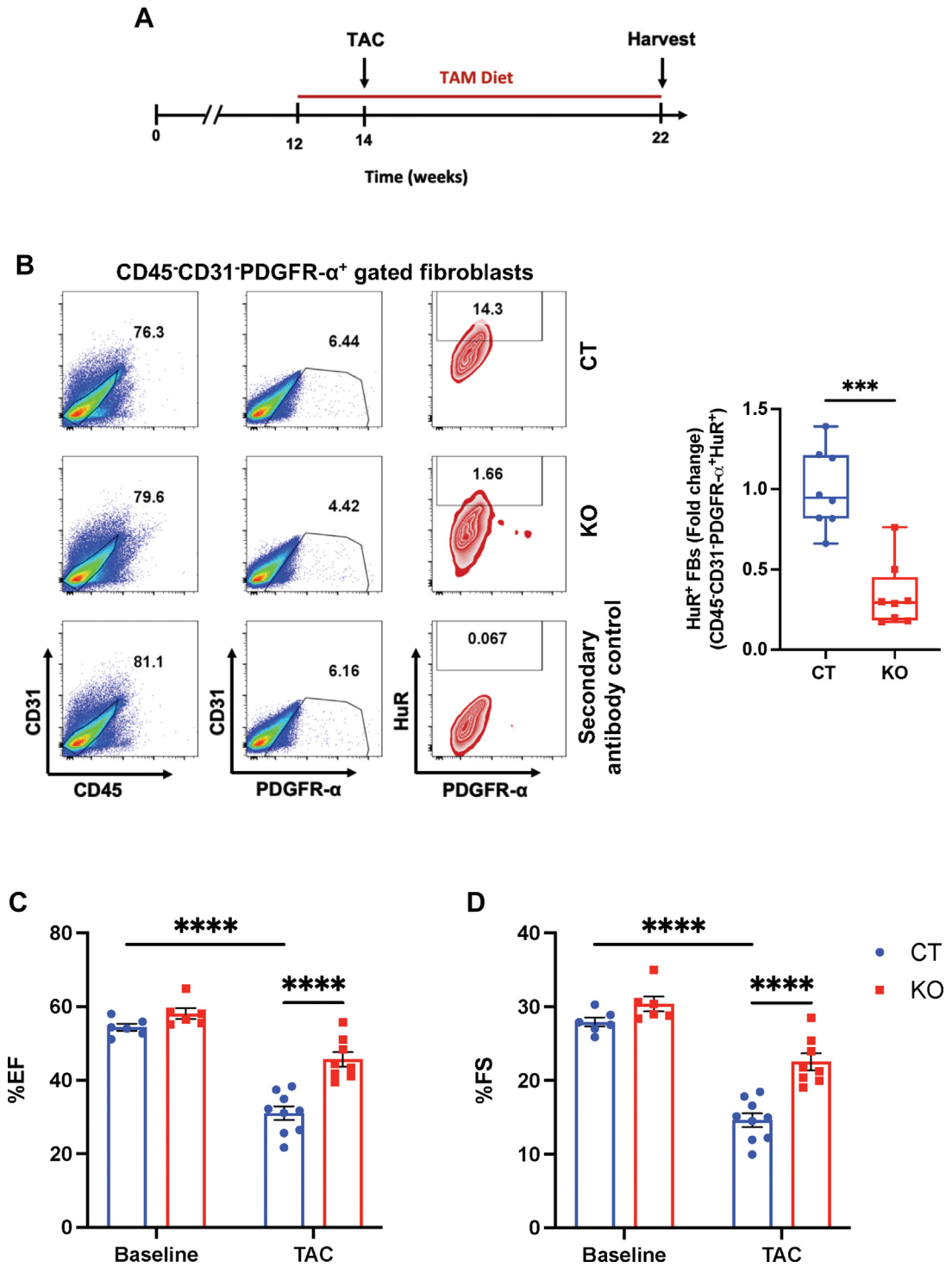

(A) Study design: 12-week-old mice were fed a tamoxifen (TAM) diet for 2 weeks before transverse aortic constriction (TAC) surgery and maintained on the TAM diet until the end of the study. (B) Flow cytometric analysis of human antigen R (HuR)-positive ($CD45^-CD31^-PDGFR\text{-}\alpha^+HuR^+$) cardiac fibroblasts (FBs) after 8 weeks of TAC. Left panel: representative flow images for $CD45^-CD31^-PDGFR\text{-}\alpha^+$–gated fibroblasts. Fluorescence-tagged secondary antibody was used as a control for intracellular staining of HuR (denoted as secondary antibody control). Right panel: quantification of $CD45^-CD31^-PDGFR\text{-}\alpha^+HuR^+$ fibroblasts in control (CT) and knockout (KO) mice (CT, n = 8; KO, n = 8, ***$P < 0.001$ vs CT mice). Values are median with 25th and 75th percentiles and were analyzed with the Mann-Whitney *U* test. Evaluation of cardiac parameters by echocardiography: ejection fraction (EF) (****$P < 0.0001$ vs CT) (C) and fractional shortening (FS) (****$P < 0.0001$ vs CT) (D). Values are mean ± SEM (CT, n > 5; KO, n > 5) and were analyzed by using a two-way analysis of variance with Tukey post hoc analysis. PDGFR-α = platelet-derived growth factor receptor-α.

JACC: BASIC TO TRANSLATIONAL SCIENCE VOL. 9, NO. 6, 2024
JUNE 2024:754–770

TABLE 1 Echocardiographic Parameters of CT and KO Mice 8 Weeks After TAC

	CT (TAC)	KO (TAC)	*P* Value
Heart rate, beats/min	455.57 ± 12.06	437.07 ± 10.39	0.27
LV mass corrected, mg	127.03 ± 8.84	93.90 ± 8.54	0.017
LVIDs, mm	3.92 ± 0.13	3.37 ± 0.14	0.012
LVIDd, mm	4.58 ± 0.11	4.15 ± 0.14	0.03
LVAWs, mm	1.05 ± 0.04	1.06 ± 0.05	0.78
LVAWd, mm	0.88 ± 0.03	0.77 ± 0.04	0.043
LVPWs, mm	0.83 ± 0.05	0.87 ± 0.05	0.61
LVPWd, mm	0.80 ± 0.04	0.74 ± 0.05	0.40

Values are mean ± SEM and were analyzed by using an unpaired Student's *t*-test.

CT = control; KO = knockout; LV = left ventricular; LVIDd = left ventricular internal diameter end-diastole; LVIDs = left ventricular internal diameter end-systole; LVAWd = left ventricular anterior wall end diastole; LVAWs = left ventricular anterior wall end systole; LVPWd = left ventricular posterior wall end diastole; LVPWs = left ventricular posterior wall end-systole; TAC = transverse aortic constriction.

the KO mice (Figure 4B) indicates that HuR deletion prevents the progression of adverse fibrosis by limiting the expansion of myofibroblasts. The expression of Collagen type I alpha 1 chain (COL1A1) was markedly reduced in HuR KO mice compared with CT mice (Figure 4C). A decline in cardiac Collagen type III alpha 1 chain (COL3A1) expression (Figure 4D) after the deletion of HuR was also observed.

In a separate experiment, cardiac fibroblasts were isolated from CT and KO mice 8 weeks after TAC. Isolated cardiac fibroblasts were enriched to remove leukocytes and endothelial cells. qRT-PCR analysis from the enriched fibroblasts revealed a significant reduction in the expression of myofibroblast markers (α-SMA, periostin, and vimentin) in the KO mice compared with the CT mice (Figure 4E). These

FIGURE 3 Effects of Myofibroblast HuR Depletion on Cardiac Hypertrophy in TAC Injury

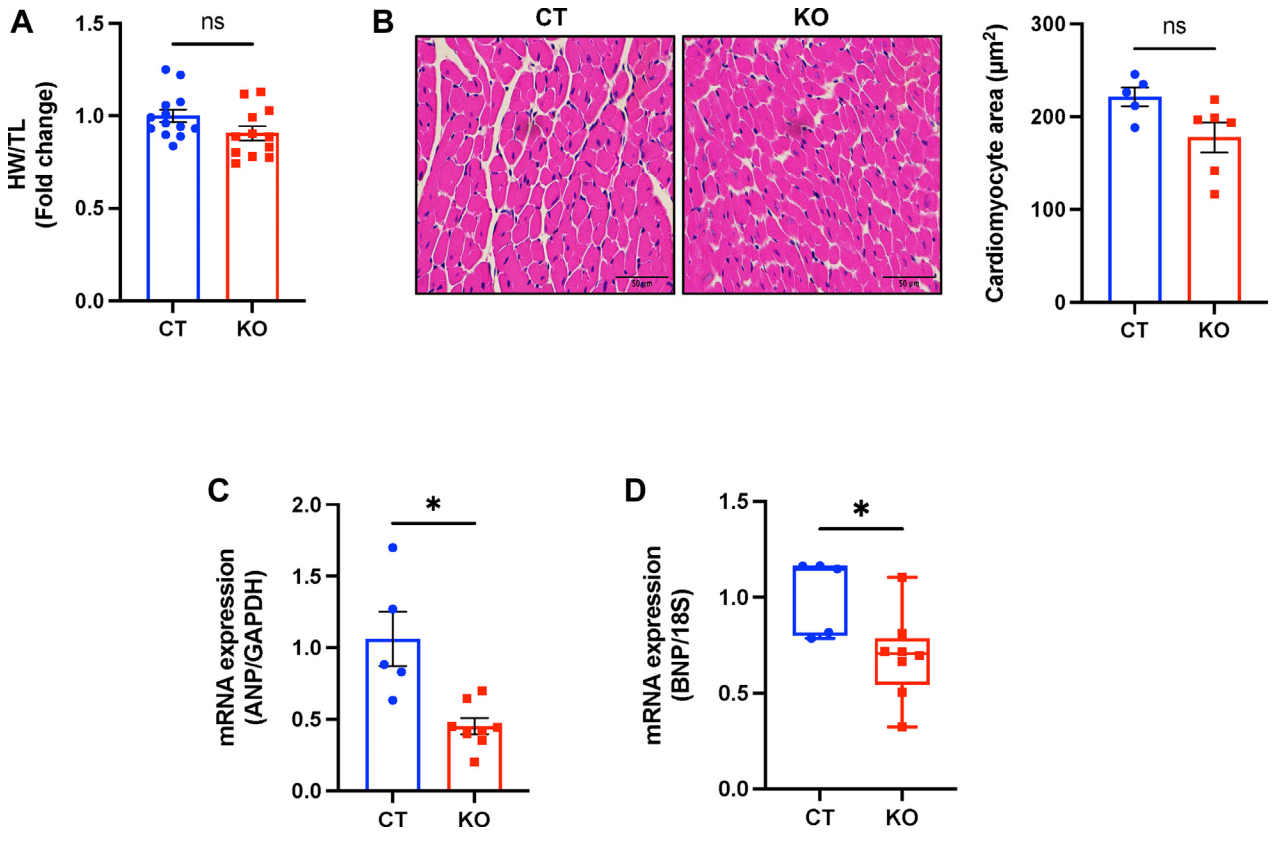

(A) Heart weight (HW) to tibia length (TL) ratio (CT, n = 13; KO, n = 12). (B) Quantification of cardiomyocyte cross-sectional area after 8 weeks of TAC surgery. Left panel: representative images of hematoxylin and eosin staining; right panel: quantification of cardiomyocyte area (CT, n = 5; KO, n =6). (C) Cardiac mRNA expression of atrial natriuretic peptide (ANP) normalized to GAPDH (CT, n = 5; KO, n = 8; *$P < 0.05$ vs CT). (D) Myocardial mRNA expression of B-type natriuretic peptide (BNP) normalized to 18S (CT, n = 5; KO, n = 8; *$P < 0.05$ vs CT). Data in A and B are presented as mean ± SEM and were analyzed by using an unpaired Student's *t*-test. Data in C are presented as mean ± SEM and were analyzed by using unpaired Welch's *t*-test. Data in D are presented as the median with 25th and 75th percentiles and were compared with the Mann-Whitney *U* test. ns = not significant; other abbreviations as in Figures 1 and 2.

FIGURE 4 Myofibroblast HuR Promotes Myocardial Fibrosis in Pressure Overload Injury

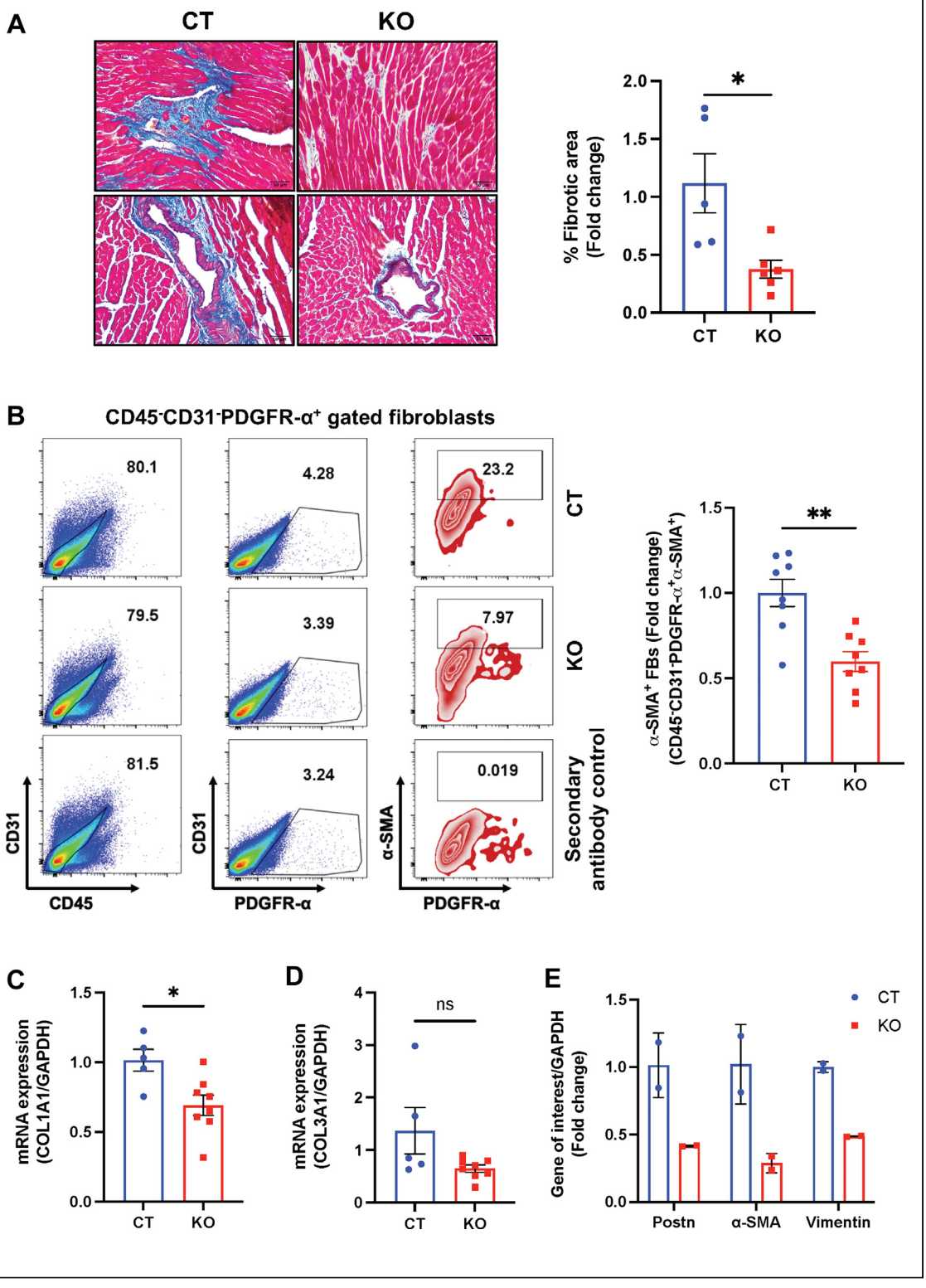

Continued on the next page

findings suggest that deletion of HuR in myofibroblasts impairs their function and prevents pathologic cardiac remodeling.

HuR PROMOTES THE PROLIFERATION OF CARDIAC MYOFIBROBLASTS AFTER INJURY. Upon activation of fibroblasts, various signaling pathways and cell cycle-related genes are up-regulated, leading to highly proliferative capacity.[36] To assess whether deletion of HuR affects the proliferation of fibroblasts after heart injury, we performed in vivo BrdU labeling and a cell proliferation assay using flow cytometry. Interestingly, the deletion of HuR compromised the proliferation of $CD31^{-}CD45^{-}\alpha\text{-}SMA^{+}BrdU^{+}$ cells in the myocardium of KO mice 1 week after TAC surgery (**Figure 5A**). Our in vitro experiments also confirmed a significant decrease in the proliferation of TGF-β1-treated HCFs in the siHuR group compared with the siControl group (**Figure 5B**). Moreover, expression of the proliferation antigen Ki67 was diminished markedly after HuR knockdown in TGF-β1-stimulated HCFs (**Figure 5C**).

HuR modulates cell proliferation by regulating cell cycle genes such as cyclins.[37,38] Based on the available literature, we sought to investigate whether HuR promotes the proliferation of activated fibroblasts by modulating the levels of cyclins. Our computational analysis[31,32] identified the presence of ARE (AUUUA pentamer sequence) in the 3′-UTR of CCND1, CCNA2, and CCNB1 mRNAs. The presence of AUUUA pentamers (Supplemental Figure 5A) and HuR-binding sites (Supplemental Figure 5B) predicted by using ViennaRNA Websuite[33] is shown in the 3′-UTR of CCND1. To validate whether HuR protein physically interacts with these cyclins, we performed an RNA-immunoprecipitation assay using IgG or anti-HuR antibodies. Conceivably, the RNA fractions of CCND1 (**Figure 6A**), CCNA2, and CCNB1 (Supplemental Figure 5C) were immunoprecipitated with anti-HuR antibody compared with IgG. Moreover, CCNE1 RNA fraction was also immunoprecipitated with anti-HuR, even though we did not find AUUUA pentamer sequences in the 3′-UTR of CCNE1.

Because HuR interacts with cyclins, we assessed whether HuR affects their mRNA stability in HCFs treated with TGF-β1. Interestingly, CCND1 and CCNA2 mRNA fractions were reduced over time in the siHuR group compared with the siControl group (**Figures 6B and 6C**), but we did not observe appreciable changes in RNA decay of CCNE1 and CCNB1 between the 2 groups (Supplemental Figures 5D and 5E). Next, we examined the effect of HuR depletion on the expression of cyclins in activated CFs. The expression of CCND1 and CCNA2 was down-regulated prominently after HuR knockdown (**Figures 6D to 6F**); however, levels of CCNE1 and CCNB1 were not altered (Supplemental Figures 5F to 5H).

We next examined whether mitogen-activated protein kinase signaling (p38 and ERK1/2) is being affected in activated fibroblasts after HuR knockdown. The phosphorylation as well as expression levels of p38 and ERK1/2 were not altered in siHuR HCFs compared with the siControl after TGF-β1 treatment (Supplemental Figure 6). Reported evidence suggests that p38 and ERK1/2 act upstream of HuR and regulate its phosphorylation.[39-41] This could be a possible explanation for the lack of alteration in their expression after HuR knockdown in activated fibroblasts.

Overall, our findings strongly support the critical role of myofibroblast-specific HuR in myofibroblast differentiation and proliferation after cardiac injury.

DISCUSSION

The current study sheds new light on the myofibroblast-specific role of the RBP HuR during heart injury. To our knowledge, we have generated

FIGURE 4 Continued

(A) Assessment of cardiac fibrosis by Masson's trichrome staining after 8 weeks of TAC surgery. Left panel: representative trichrome-stained left ventricular regions showing interstitial and perivascular fibrosis; right panel: quantification of left ventricular fibrosis (CT, n = 5; KO, n = 6; $*P < 0.05$ vs CT). (B) Flow cytometric assessment of $CD45^{-}CD31^{-}PDGFR\text{-}\alpha^{+}\alpha\text{-}SMA^{+}$ fibroblasts in the left ventricles of CT and KO mice. Left panel: representative flow images for $CD45^{-}CD31^{-}PDGFR\text{-}\alpha^{+}$–gated fibroblasts. Fluorescence-tagged secondary antibody was used as a control for intracellular staining of α-SMA (denoted as secondary antibody control). Right panel: quantification of $CD45^{-}CD31^{-}PDGFR\text{-}\alpha^{+}\alpha\text{-}SMA^{+}$ fibroblasts in CT and KO mice (CT, n = 8; KO, n = 8; $**P < 0.01$ vs CT). Myocardial gene expression of Collagen type I alpha 1 chain (COL1A1) (C) and Collagen type III alpha 1 chain (COL3A1) (D) in the left ventricles of CT and KO mice normalized to GAPDH (CT, n = 5; KO, n = 8; COL1A1: $*P < 0.05$, COL3A1: P = ns vs CT). (E) Real-time quantitative polymerase chain reaction analysis of myofibroblast markers (periostin [Postn], α-SMA, and vimentin) in enriched cardiac fibroblasts of CT and KO mice after 8 weeks of TAC surgery (n = 3 mice per group per experiment; the samples were pooled and repeated twice). Values are mean ± SEM. Data in A and D were analyzed by using an unpaired Welch's *t*-test. Data in B and C were analyzed by using an unpaired Student's *t*-test. Abbreviations as in **Figures 1 to 3**.

FIGURE 5 Deletion of HuR Reduces Cardiac Myofibroblast Proliferation After Injury

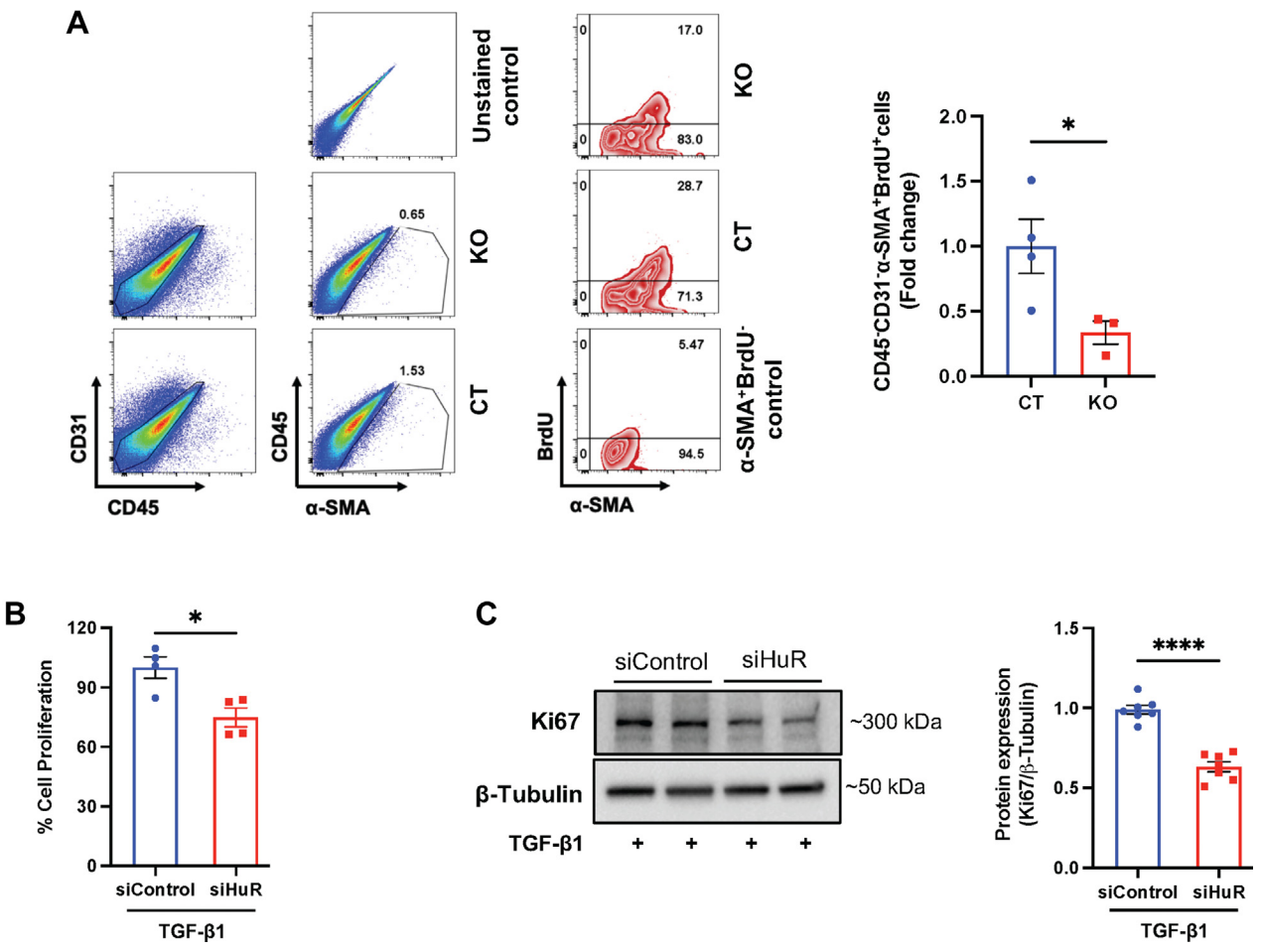

(A) Flow cytometric analysis of $CD31^{-}CD45^{-}\alpha\text{-}SMA^{+}BrdU^{+}$ cells in the heart of the CT and KO mice after 1 week of TAC injury using 5-bromo-2′-deoxyuridine (BrdU) labeling. Left panel: representative flow cytometry images. Right panel: quantification of $CD45^{-}CD31^{-}\alpha\text{-}SMA^{+}BrdU^{+}$ cells in CT and KO mice (CT, n = 4; KO, n = 3; $^{*}P < 0.05$ vs CT; BrdU administration: 10 mg/kg body weight). (B) In vitro cell proliferation was measured by using the MTT assay in siControl and siHuR HCFs treated with TGF-β1 for 48 hours (n = 4 per group; $^{*}P < 0.05$ vs siControl). (C) Expression of Ki67 was assessed by using Western blot analysis in siControl and siHuR HCFs treated with TGF-β1 for 24 hours and normalized to β-tubulin (n > 5/group; $^{****}P < 0.0001$ vs siControl). Values are mean ± SEM and were analyzed by using an unpaired Student's *t*-test. Abbreviations as in Figures 1 and 2.

the first myofibroblast-specific conditional HuR KO mouse to show the direct role of HuR in myofibroblast biology and function after cardiac insult. In this study, we found that the deletion of HuR in myofibroblasts limits their proliferation and minimizes pathologic fibrotic remodeling and cardiac dysfunction in pressure overload-induced cardiac injury.

In the case of any cardiac insult, quiescent cardiac fibroblasts rapidly respond to changes in the neighboring microenvironment.[1,2] Fibroblast-to-myofibroblast differentiation is a key event in the initiation of fibrosis, and posttranscriptional mechanisms are important in TGF-β1-mediated fibroblast-to-myofibroblast conversion in the heart. In one study,[4] genome-wide transcriptional and translational changes were examined in TGF-β1-stimulated primary HCFs, and approximately one-third of differential gene expression in activated fibroblasts was subjected to translational regulation. The authors also showed that RBPs are key players in the post-transcriptional regulation of myofibroblast differentiation and could be explored as potential therapeutic targets.

As an RBP, HuR binds to ARE regions in the 3′-UTR of various mRNAs and promotes their stability and subsequent translation.[8,9,11] HuR-dependent

FIGURE 6 Deletion of HuR Reduces the Levels of Cyclins D1 and A2 in Activated Cardiac Fibroblasts

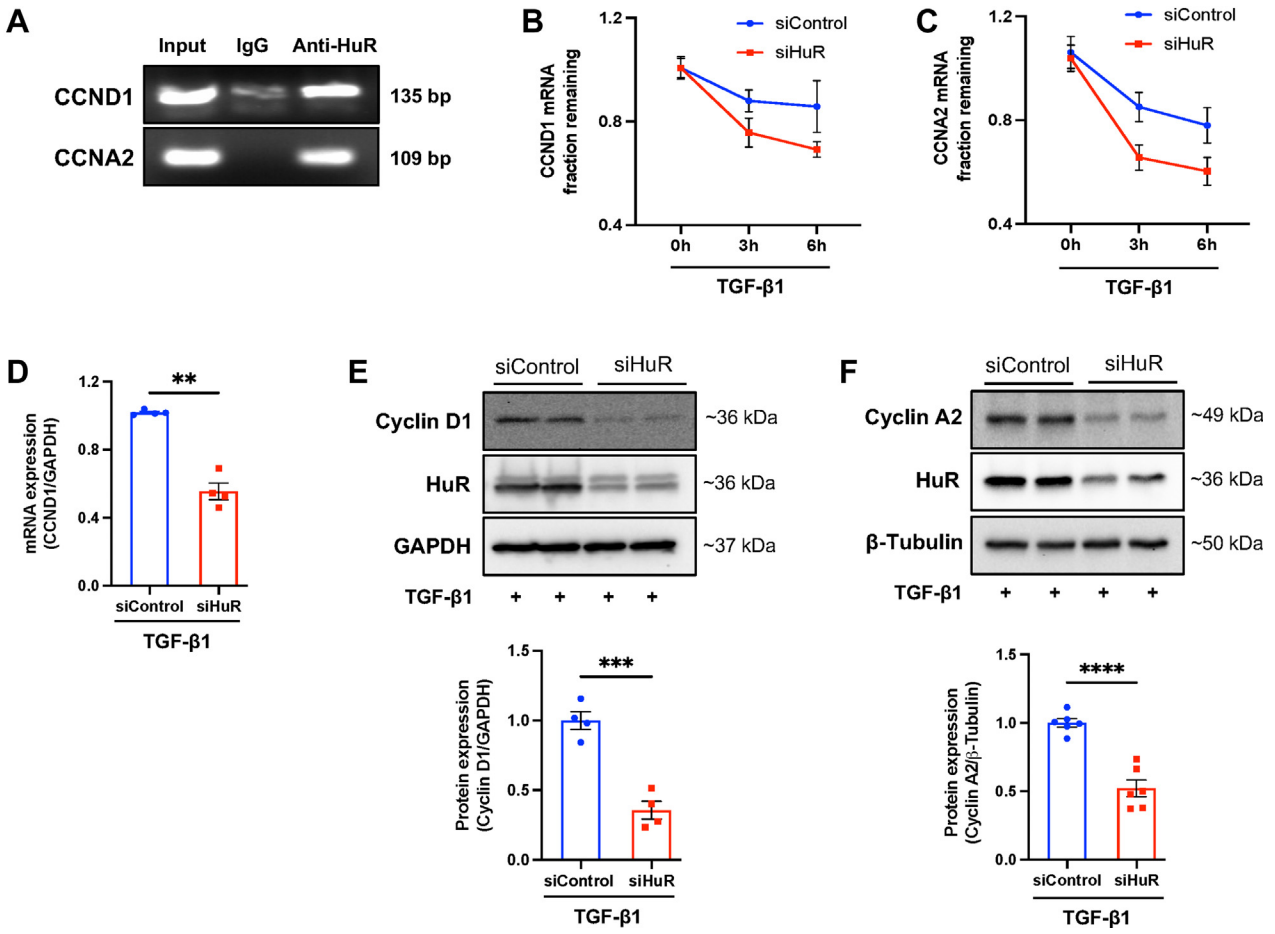

(A) An RNA immunoprecipitation assay to assess the interaction of HuR with cyclin D1 (CCND1) and cyclin A2 (CCNA2). The CCND1 (amplicon size: approximately 135 bp) and CCNA2 (amplicon size: approximately 109 bp) RNA fractions were immunoprecipitated by using immunoglobulin G (IgG) or anti-HuR antibodies and were amplified by polymerase chain reaction. The mRNA stability of CCND1 (B) and CCNA2 (C) was evaluated in TGF-β1–treated siControl or siHuR HCFs using an actinomycin D chase assay. (D) CCND1 mRNA expression was analyzed in TGF-β1–treated siControl and siHuR HCFs for 24 hours and normalized to GAPDH (n = 4 per group; $^{**}P < 0.01$ vs siControl). (E) CCND1 and HuR expression was assessed by Western blot analysis in TGF-β1–treated siControl and siHuR HCFs for 24 hours and normalized to GAPDH (n = 4 per group; $^{***}P < 0.001$ vs siControl). (F) Protein expression of CCNA2 in TGF-β1–stimulated siControl and siHuR HCFs for 24 hours and normalized to β-tubulin (n > 5 per group, $^{****}P < 0.0001$ vs siControl). Top panel: representative immunoblots. Bottom panel: densitometric analysis of cyclin expression. Values are mean ± SEM. The mRNA stability of CCND1 (B) and CCNA2 (C) was analyzed by using a 2-way repeated measures analysis of variance with Šidák multiple comparisons test. Data in D were analyzed by using an unpaired Welch's *t*-test. Data in E and F were analyzed by using an unpaired Student's *t*-test. Abbreviations as in Figures 1 and 2.

regulation of cancer progression and pathology has been extensively studied,[42] while its role in fibrosis is slowly evolving. Multiple studies have recognized that HuR imparts critical functions in the pathogenesis of pulmonary,[14] hepatic,[12] and renal[13] fibrosis. In the context of heart injuries, our laboratory has previously reported that the up-regulation of HuR in diabetic and ischemic hearts could be a plausible cause of cardiac remodeling.[16-18,43] Furthermore, a previous study described the pathologic significance of HuR in cardiac remodeling, in which HuR was identified as a novel mediator of cardiac hypertrophy in isolated rat cardiomyocytes.[39] The Tranter laboratory also reported that HuR deletion protects against cardiac remodeling and fibrosis in an inducible cardiomyocyte-specific HuR knockout mouse subjected to pressure overload injury.[15] Despite the strong association between HuR and cardiac

remodeling, an explicit role of HuR in myofibroblast biology and resultant fibrosis response was lacking. We previously observed that upon cardiac injury, HuR was predominantly localized to the border zone of infarct, specifically in fibroblast-like cells.[17] Therefore, the current study was designed to test the direct involvement of HuR in myofibroblast function in heart disease.

We first stimulated primary adult mouse cardiac fibroblasts and HCFs with TGF-β1 to initiate fibroblast-to-myofibroblast differentiation, a process that is key to cardiac fibrosis.[34] Our data showed that the expression of HuR was significantly increased in activated myofibroblasts. To investigate the role of HuR in myofibroblasts, we performed a series of molecular and functional assays and found that the knockdown of HuR reduced myofibroblast differentiation and lowered the expression of fibrotic genes. Our findings are supported by a recent study[19] in which the authors showed that HuR expression was significantly higher in myofibroblasts compared with quiescent fibroblasts and nonstressed cardiomyocytes. The authors also showed that HuR is responsible for the TGF-β1-mediated activation of cardiac myofibroblast by posttranscriptional modulation of WISP-1. Based on these in vitro data, we generated a novel tamoxifen-inducible periostin-Cre-driven myofibroblast-specific HuR KO mouse to evaluate the therapeutic potential of targeting HuR in vivo.

Baseline characterization of cardiac functions in these mice did not show any changes compared with wild-type mice. However, myofibroblast-specific deletion of HuR preserved cardiac functions in KO mice after TAC-induced pressure overload. We also observed significant inhibition of myocardial fibrosis, reduction in collagen deposition, and lower expression of extracellular matrix molecules in KO mice compared with CT mice. In addition, deletion of HuR restricted the expansion of PDGFR-$\alpha^{+}\alpha$-SMA^{+} fibroblasts after heart injury. Notably, evaluation of cardiac hypertrophy revealed a significant reduction in the expression of atrial natriuretic peptide and B-type natriuretic peptide after HuR deletion in TAC injury, suggesting that depletion of HuR in activated fibroblasts also abrogates cardiac hypertrophy response.

It is well known that cardiac fibroblasts and cardiomyocytes interact via paracrine signaling, mechanical and extracellular matrix interactions, and gap junctions, affecting cardiac homeostasis and function.[44,45] In diseased hearts, soluble mediators and paracrine signaling drive indirect cross-talk between cardiac fibroblasts and cardiomyocytes to affect disease pathogenesis. Angiotensin II and TGF-β1, potent profibrotic mediators, are secreted by cardiac (myo)fibroblasts and are widely reported to induce fibrosis, cardiomyocyte hypertrophy, and cardiac remodeling.[44,46-48] Furthermore, interleukins, expressed by cardiomyocytes and fibroblasts, reportedly regulate both cell types. IL-6, secreted by both cardiomyocytes and cardiac fibroblasts, contributes to cardiomyocyte hypertrophy and cardiac fibrosis.[44,46,49] Conversely, IL-33, secreted by fibroblasts, prevents cardiomyocyte hypertrophy in response to angiotensin II treatment and pressure overload.[50] It is also well established that excessive collagen deposition impairs cardiomyocyte contractility and function.[51] TGF-β1 and HuR induce each other's expression in a positive feedback loop,[35] and TGF-β1 induces hypertrophic effects.[44,52] Based on these studies, we speculate that the deletion of HuR in myofibroblasts may also modulate hypertrophic response via crosstalk with cardiomyocytes.

Our investigation also showed reduced proliferation of CD31^{-}CD45^{-}α-SMA^{+} cells in the heart of HuR KO mice after TAC surgery. The critical role of HuR in cell proliferation by regulating mRNA stability of cyclins,[37] modulation of the G1/S phase transition,[38] and regulation of DNA damage checkpoint[38] is well known. Our computational and RNA-immunoprecipitation studies showed that HuR interacts with cyclins A2, B1, D1, and E1 in activated fibroblasts. Interestingly, deletion of HuR exhibited appreciable reduction in CCND1 and CCNA2 (but not in CCNB1 and CCNE1) mRNA stability in the actinomycin D chase experiment. Furthermore, depletion of HuR significantly abrogated the expression of CCND1 and CCNA2 in activated HCFs, indicating that HuR could promote myofibroblast proliferation through modulation of cell cycle. Altogether our findings suggest that myofibroblast-specific HuR regulates both myofibroblast differentiation and proliferation after cardiac injury (**Figure 7**).

STUDY LIMITATIONS. First, we identified fibroblast proliferation as one of the mechanisms, however, several other mechanistic signaling factors might be involved, and therefore further screening approaches are warranted for a comprehensive mechanistic analysis. Second, it is imperative to investigate the effect of myofibroblast HuR deletion on other cell types in the heart such as cardiomyocytes and endothelial cells. Next, cardiac

FIGURE 7 Schematic Illustration of HuR-Mediated Regulation of Myofibroblast Differentiation and Proliferation

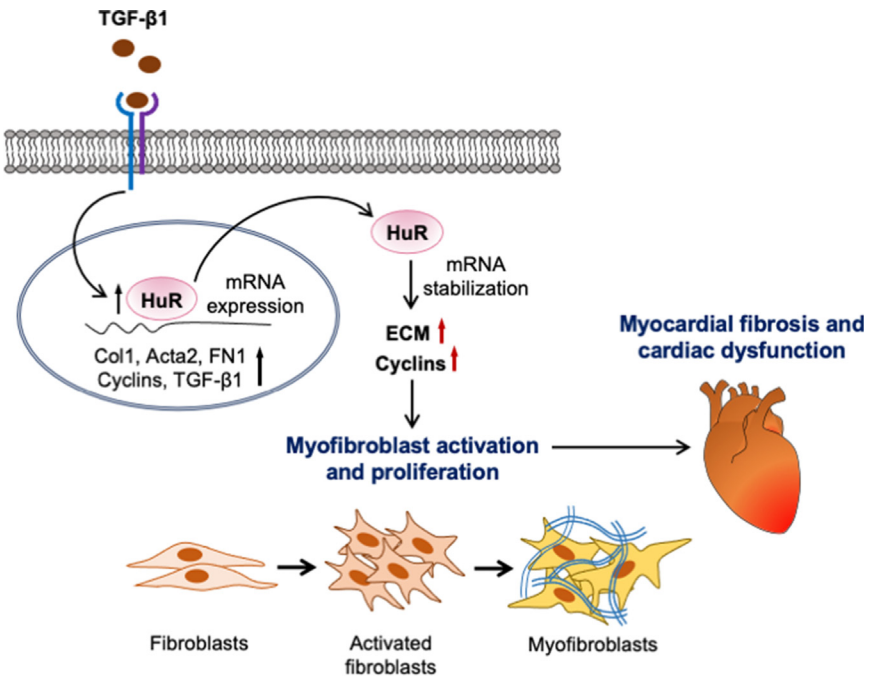

During cardiac injury, TGF-β1 stimulation activates the expression of fibroblast HuR in a positive feedback manner. Activation of HuR induces mRNA expression and stability of extracellular matrix (ECM) and cell cycle–related genes to promote fibroblast-to-myofibroblast differentiation and proliferation that leads to pathologic remodeling and cardiac dysfunction. Depletion of myofibroblast HuR prevented activation and proliferation of activated fibroblasts, alleviated cardiac fibrosis, and restored cardiac function during pressure overload injury. Acta2 = actin alpha 2, smooth muscle; Col1 = collagen type I; FN1 = fibronectin; other abbreviations as in Figure 1.

toxicity of constitutive or transiently active Cre is reported in cardiomyocyte-specific lines,[53,54] which could lead to misinterpretation of data. Although side effects of Cre recombinase can be minimized by its transient expression and dose adjustment of tamoxifen, it cannot be ruled out. Thus, including nonfloxed MCM$^{+/-}$ CT mice in the study would be ideal.[55] In the current study, we cannot exclude any confounding effects of Cre recombinase in the presence of tamoxifen. However, we observed a protective phenotype in HuR$^{fl/fl}$/Cre$^{+/-}$/tamoxifen mice (KO) after TAC, and therefore the outcome of the study should not change by the exclusion of nonfloxed HuR$^{WT/WT}$/Cre$^{+/-}$/tamoxifen CT mice. Finally, given the multifactorial etiology of heart failure, exploring the role of myofibroblast-specific HuR in other models of heart disease is necessary. Despite these limitations, this study highlights the critical role of myofibroblast-specific HuR in pathologic fibrosis in the injured heart.

CONCLUSIONS

The current study provides evidence that myofibroblast-specific deletion of HuR limits adverse cardiac remodeling in the injured heart, improving cardiac function. The profibrotic effects of HuR in the heart might be attributed to its ability to promote myofibroblast differentiation and proliferation through posttranscriptional regulation. Therefore, targeting HuR in myofibroblasts could be a novel pragmatic approach to limit cardiac fibrosis and heart failure.

Due to their complex structure and the absence of defined small molecule binding sites, RBPs are considered difficult molecules for drug targeting. However, in recent years, several small molecules have been screened that inhibit RBP function by modulating RBP-RNA interaction and dynamics of RBPs.[56] These small molecule inhibitors could be valuable tools for developing novel therapeutics for

various diseases. Several small molecules have also been investigated to inhibit HuR function in various diseases, especially in cancer. Small molecule inhibitors of HuR, such as MS-444, CMLD-2, and KH-3, reportedly limit cancer cell proliferation, migration, and invasion.[57-59] A recent study screened 36 new compounds and identified 2 potential candidates that inhibit HuR activity by directly binding to its RNA-binding pockets.[60] These small molecules successfully inhibited cancer cell invasion and tumor growth in the breast cancer xenograft model. KH-3, a small molecule inhibitor of HuR, has been shown to mitigate fibrosis in different organs, including cardiac fibrosis.[13,15,19,61] These studies suggest that despite the complexity of the structure and multifaceted functions of HuR, new multi-omics tools and advanced drug-targeting strategies could facilitate the development of novel HuR-dependent therapeutics for cardiac fibrosis and other pathologies.

FUNDING SUPPORT AND AUTHOR DISCLOSURES

This work was supported by National Institutes of Health grants HL116729 (Dr Krishnamurthy) and HL138023 (Drs Krishnamurthy and Zhang), an American Heart Association Transformational Project Award (19TPA34850100, Dr Krishnamurthy), and an American Heart Association postdoctoral fellowship (916497, Dr Singh). All other authors have reported that they have no relationships relevant to the contents of this paper to disclose.

ADDRESS FOR CORRESPONDENCE: Dr Prasanna Krishnamurthy, Department of Biomedical Engineering, Heersink School of Medicine and School of Engineering, University of Alabama at Birmingham, 1670 University Boulevard, Volker Hall G094, Birmingham, Alabama 35294, USA. E-mail: prasanak@uab.edu.

PERSPECTIVES

COMPETENCY IN MEDICAL KNOWLEDGE: Efficient antifibrotic therapies are currently unavailable, necessitating the discovery of new targets to combat cardiac fibrosis. RBPs are key mediators of fibroblast-to-myofibroblast differentiation. In this study, using myofibroblast-specific HuR KO mice, we show that targeting the RBP HuR presents a novel approach to combat cardiac fibrosis by efficient fibrosis resolution.

TRANSLATIONAL OUTLOOK: Our conditional myofibroblast-specific HuR KO mouse model provides a unique and innovative tool to investigate the role of HuR in pathologic fibrosis. This model may aid in developing better clinical approaches toward antifibrotic therapies.

REFERENCES

1. Frangogiannis NG. Cardiac fibrosis. *Cardiovasc Res*. 2021;117:1450–1488.

2. Travers JG, Kamal FA, Robbins J, Yutzey KE, Blaxall BC. Cardiac fibrosis. *Circ Res*. 2016;118:1021–1040.

3. Bretherton R, Bugg D, Olszewski E, Davis J. Regulators of cardiac fibroblast cell state. *Matrix Biol*. 2020;91-92:117–135.

4. Chothani S, Schäfer S, Adami E, et al. Widespread translational control of fibrosis in the human heart by RNA-binding proteins. *Circulation*. 2019;140:937–951.

5. de Bruin RG, Vogel G, Prins J, et al. Targeting the RNA-binding protein QKI in myeloid cells ameliorates macrophage-induced renal interstitial fibrosis. *Epigenomes*. 2020;4:2.

6. Zhu H, Zhang Y, Zhang C, Xie Z. RNA-binding profiles of CKAP4 as an RNA-binding protein in myocardial tissues. *Front Cardiovasc Med*. 2021;8:773573.

7. Travers JG, Tharp CA, Rubino M, McKinsey TA. Therapeutic targets for cardiac fibrosis: from old school to next-gen. *J Clin Invest*. 2022;132:e148554.

8. Lebedeva S, Jens M, Theil K, et al. Transcriptome-wide analysis of regulatory interactions of the RNA-binding protein HuR. *Mol Cell*. 2011;43:340–352.

9. Rajasingh J. The many facets of RNA-binding protein HuR. *Trends Cardiovasc Med*. 2015;25:684–686.

10. Suresh Babu S, Joladarashi D, Jeyabal P, Thandavarayan RA, Krishnamurthy P. RNA-stabilizing proteins as molecular targets in cardiovascular pathologies. *Trends Cardiovasc Med*. 2015;25:676–683.

11. Mukherjee N, Corcoran DL, Nusbaum JD, et al. Integrative regulatory mapping indicates that the RNA-binding protein HuR couples pre-mRNA processing and mRNA stability. *Mol Cell*. 2011;43:327–339.

12. Ge J, Chang N, Zhao Z, et al. Essential roles of RNA-binding protein HuR in activation of hepatic stellate cells induced by transforming growth factor-β1. *Sci Rep*. 2016;6:22141.

13. Liu S, Huang Z, Tang A, et al. Inhibition of RNA-binding protein HuR reduces glomerulosclerosis in experimental nephritis. *Clin Sci (Lond)*. 2020;134:1433–1448.

14. Al-Habeeb F, Aloufi N, Traboulsi H, et al. Human antigen R promotes lung fibroblast differentiation to myofibroblasts and increases extracellular matrix production. *J Cell Physiol*. 2021;236:6836–6851.

15. Green LC, Anthony SR, Slone S, et al. Human antigen R as a therapeutic target in pathological cardiac hypertrophy. *JCI Insight*. 2019;4:e121541.

16. Krishnamurthy P, Rajasingh J, Lambers E, Qin G, Losordo DW, Kishore R. IL-10 inhibits inflammation and attenuates left ventricular remodeling after myocardial infarction via activation of STAT3 and suppression of HuR. *Circ Res*. 2009;104:e9–18.

17. Krishnamurthy P, Lambers E, Verma S, et al. Myocardial knockdown of mRNA-stabilizing protein HuR attenuates post-MI inflammatory response and left ventricular dysfunction in IL-10-null mice. *FASEB J*. 2010;24:2484–2494.

18. Govindappa PK, Patil M, Garikipati VNS, et al. Targeting exosome-associated human antigen R attenuates fibrosis and inflammation in diabetic heart. *FASEB J*. 2020;34:2238–2251.

19. Green LC, Slone S, Anthony SR, et al. HuR-dependent expression of Wisp1 is necessary for TGFβ-induced cardiac myofibroblast activity. *J Mol Cell Cardiol*. 2023;174:38–46.

20. Fu X, Khalil H, Kanisicak O, et al. Specialized fibroblast differentiated states underlie scar

formation in the infarcted mouse heart. *J Clin Invest*. 2018;128:2127–2143.

21. Xiang F-L, Fang M, Yutzey KE. Loss of β-catenin in resident cardiac fibroblasts attenuates fibrosis induced by pressure overload in mice. *Nat Commun*. 2017;8:712.

22. Khalil H, Kanisicak O, Prasad V, et al. Fibroblast-specific TGF-β-Smad2/3 signaling underlies cardiac fibrosis. *J Clin Invest*. 2017;127:3770–3783.

23. Molkentin JD, Bugg D, Ghearing N, et al. Fibroblast-specific genetic manipulation of p38 mitogen-activated protein kinase in vivo reveals its central regulatory role in fibrosis. *Circulation*. 2017;136:549–561.

24. Kanisicak O, Khalil H, Ivey MJ, et al. Genetic lineage tracing defines myofibroblast origin and function in the injured heart. *Nat Commun*. 2016;7:12260.

25. Acharya A, Baek ST, Banfi S, Eskiocak B, Tallquist MD. Efficient inducible Cre-mediated recombination in Tcf21 cell lineages in the heart and kidney. *Genesis*. 2011;49:870–877.

26. Ghosh M, Aguila HL, Michaud J, et al. Essential role of the RNA-binding protein HuR in progenitor cell survival in mice. *J Clin Invest*. 2009;119:3530–3543.

27. Umbarkar P, Tousif S, Singh AP, et al. Fibroblast GSK-3α promotes fibrosis via RAF-MEK-ERK pathway in the injured heart. *Circ Res*. 2022;131:620–636.

28. Patil M, Saheera S, Dubey PK, et al. Novel mechanisms of exosome-mediated phagocytosis of dead cells in injured heart. *Circ Res*. 2021;129:1006–1020.

29. Suarez-Arnedo A, Torres Figueroa F, Clavijo C, Arbeláez P, Cruz JC, Muñoz-Camargo C. An image J plugin for the high throughput image analysis of in vitro scratch wound healing assays. *PLoS One*. 2020;15:e0232565.

30. Dubey S, Dubey PK, Umeshappa CS, Ghebre YT, Krishnamurthy P. Inhibition of RUNX1 blocks the differentiation of lung fibroblasts to myofibroblasts. *J Cell Physiol*. 2022;237:2169–2182.

31. Bakheet T, Hitti E, Khabar KSA. ARED-Plus: an updated and expanded database of AU-rich element-containing mRNAs and pre-mRNAs. *Nucleic Acids Res*. 2018;46:D218–D220.

32. Fallmann J, Sedlyarov V, Tanzer A, Kovarik P, Hofacker IL. AREsite2: an enhanced database for the comprehensive investigation of AU/GU/U-rich elements. *Nucleic Acids Res*. 2016;44:D90–D95.

33. Gruber AR, Lorenz R, Bernhart SH, Neuböck R, Hofacker IL. The Vienna RNA Websuite. *Nucleic Acids Res*. 2008;36:W70–W74.

34. Meng X-M, Nikolic-Paterson DJ, Lan HY. TGF-β: the master regulator of fibrosis. *Nat Rev Nephrol*. 2016;12:325–338.

35. Bai D, Gao Q, Li C, Ge L, Gao Y, Wang H. A conserved TGFβ1/HuR feedback circuit regulates the fibrogenic response in fibroblasts. *Cell Signal*. 2012;24:1426–1432.

36. Gibb AA, Lazaropoulos MP, Elrod JW. Myofibroblasts and fibrosis: mitochondrial and metabolic control of cellular differentiation. *Circ Res*. 2020;127:427–447.

37. Wang W, Caldwell MC, Lin S, Furneaux H, Gorospe M. HuR regulates cyclin A and cyclin B1 mRNA stability during cell proliferation. *EMBO J*. 2000;19:2340–2350.

38. Osma-Garcia IC, Capitan-Sobrino D, Mouysset M, et al. The RNA-binding protein HuR is required for maintenance of the germinal centre response. *Nat Commun*. 2021;12:6556.

39. Slone S, Anthony SR, Wu X, et al. Activation of HuR downstream of p38 MAPK promotes cardiomyocyte hypertrophy. *Cell Signal*. 2016;28:1735–1741.

40. Lafarga V, Cuadrado A, Lopez de Silanes I, Bengoechea R, Fernandez-Capetillo O, Nebreda AR. p38 Mitogen-activated protein kinase- and HuR-dependent stabilization of p21(Cip1) mRNA mediates the G(1)/S checkpoint. *Mol Cell Biol*. 2009;29:4341–4351.

41. Cheng M, Yang L, Fan M, An S, Li J. Proatherogenic stimuli induce HuR in atherosclerosis through MAPK/ErK pathway. *Am J Transl Res*. 2019;11:2317–2327.

42. Wang J, Guo Y, Chu H, Guan Y, Bi J, Wang B. Multiple functions of the RNA-binding protein HuR in cancer progression, treatment responses and prognosis. *Int J Mol Sci*. 2013;14:10015–10041.

43. Jeyabal P, Thandavarayan RA, Joladarashi D, et al. MicroRNA-9 inhibits hyperglycemia-induced pyroptosis in human ventricular cardiomyocytes by targeting ELAVL1. *Biochem Biophys Res Commun*. 2016;471:423–429.

44. Hall C, Gehmlich K, Denning C, Pavlovic D. Complex relationship between cardiac fibroblasts and cardiomyocytes in health and disease. *J Am Heart Assoc*. 2021;10:e019338.

45. Pellman J, Zhang J, Sheikh F. Myocyte-fibroblast communication in cardiac fibrosis and arrhythmias: mechanisms and model systems. *J Mol Cell Cardiol*. 2016;94:22–31.

46. Nicin L, Wagner JUG, Luxán G, Dimmeler S. Fibroblast-mediated intercellular crosstalk in the healthy and diseased heart. *FEBS Lett*. 2022;596:638–654.

47. Sun Y, Zhang JQ, Zhang J, Ramires FJ. Angiotensin II, transforming growth factor-beta1 and repair in the infarcted heart. *J Mol Cell Cardiol*. 1998;30:1559–1569.

48. Schieffer B, Wirger A, Meybrunn M, et al. Comparative effects of chronic angiotensin-converting enzyme inhibition and angiotensin II type 1 receptor blockade on cardiac remodeling after myocardial infarction in the rat. *Circulation*. 1994;89:2273–2282.

49. Banerjee I, Fuseler JW, Intwala AR, Baudino TA. IL-6 loss causes ventricular dysfunction, fibrosis, reduced capillary density, and dramatically alters the cell populations of the developing and adult heart. *Am J Physiol Heart Circ Physiol*. 2009;296:H1694–H1704.

50. Sanada S, Hakuno D, Higgins LJ, Schreiter ER, McKenzie ANJ, Lee RT. IL-33 and ST2 comprise a critical biomechanically induced and cardioprotective signaling system. *J Clin Invest*. 2007;117:1538–1549.

51. Rohr S. Arrhythmogenic implications of fibroblast-myocyte interactions. *Circ Arrhythm Electrophysiol*. 2012;5:442–452.

52. Cartledge JE, Kane C, Dias P, et al. Functional crosstalk between cardiac fibroblasts and adult cardiomyocytes by soluble mediators. *Cardiovasc Res*. 2015;105:260–270.

53. Buerger A, Rozhitskaya O, Sherwood MC, et al. Dilated cardiomyopathy resulting from high-level myocardial expression of Cre-recombinase. *J Card Fail*. 2006;12:392–398.

54. Koitabashi N, Bedja D, Zaiman AL, et al. Avoidance of transient cardiomyopathy in cardiomyocyte-targeted tamoxifen-induced MerCreMer gene deletion models. *Circ Res*. 2009;105:12–15.

55. Hougen K, Aronsen JM, Stokke MK, et al. Cre-loxP DNA recombination is possible with only minimal unspecific transcriptional changes and without cardiomyopathy in Tg(alphaMHC-MerCreMer) mice. *Am J Physiol Heart Circ Physiol*. 2010;299:H1671–H1678.

56. Li Q, Kang C. Targeting RNA-binding proteins with small molecules: perspectives, pitfalls and bifunctional molecules. *FEBS Lett*. 2023;597:2031–2047.

57. Muralidharan R, Mehta M, Ahmed R, et al. HuR-targeted small molecule inhibitor exhibits cytotoxicity towards human lung cancer cells. *Sci Rep*. 2017;7:9694.

58. Blanco FF, Preet R, Aguado A, et al. Impact of HuR inhibition by the small molecule MS-444 on colorectal cancer cell tumorigenesis. *Oncotarget*. 2016;7:74043–74058.

59. Wu X, Gardashova G, Lan L, et al. Targeting the interaction between RNA-binding protein HuR and FOXQ1 suppresses breast cancer invasion and metastasis. *Commun Biol*. 2020;3:193.

60. Wu X, Ramesh R, Wang J, et al. Small molecules targeting the RNA-binding protein HuR inhibit tumor growth in xenografts. *J Med Chem*. 2023;66:2032–2053.

61. Huang Z, Liu S, Tang A, et al. Targeting RNA-binding protein HuR to inhibit the progression of renal tubular fibrosis. *J Transl Med*. 2023;21:428.

KEY WORDS cardiac fibrosis, heart failure, human antigen R, left ventricular remodeling, myofibroblasts

APPENDIX For supplemental figures and tables, please see the online version of this paper.